Transport and deposition of fine sediment in a channel partly covered by flexible vegetation

Walter Box[1,*], *Kaisa* Västilä[1], and *Juha* Järvelä[1]
[1]Department of Built Environment, Aalto University School of Engineering, Espoo, Finland.

Abstract. Riparian plants exert flow resistance and largely influence the flow structure, which affects erosion, deposition and transport processes of fine sediments. Predicting these vegetative effects is important for flood, sediment and nutrient management. However, predictions on the fate of sediments are complicated by uncertainties associated with the suitable parameterization of natural plants and the associated effects on the turbulent flow field and on the variables in the transport equations. The aim of this study is to quantify deposition and transport of fine sandy sediment in a partly vegetated channel under laboratory conditions. Care was taken to reproduce conditions typical of vegetated floodplain flows including dense flexible grassy understory as a starting point. The experiments were conducted in a flume that is specifically designed to recirculate fine sediment. We measured suspended sediment concentrations with optical turbidity sensors and determined patterns of net deposition over the vegetated parts of the cross section. The flow field was determined with acoustic Doppler velocimetry. Our investigations are intended to improve future predictions of fine sediment storage and transport in natural or constructed vegetated channels, and the first results reported herein were useful in designing further, on-going experiments with complex combinations of vegetation and channel geometry. Key words: sediment transport, suspended sediment, deposition, riparian vegetation, flow field.

1. Introduction

Transport and deposition of fine sediment have important implications on determining the quality of environment, and consequently, on assessing possible actions required to reduce or mitigate environmental problems. In recent research, important advances on the effect of vegetation on the transport processes of suspended sediment (SS, e.g. fine cohesive and non-cohesive sediments) and solutes have been gained, though mostly assuming plants behaving as rigid cylinders. For example, Zong and Nepf [1] explained the spatial pattern of net deposition within an emergent patch of vegetation through the interplay between advection and lateral dispersion of the particles. However, in nature plants are typically non-cylindrical, consist mostly of flexible material (e.g. mostly leaves, less flexible stems and branches), and many properties vary temporally (e.g. seasonal differences due to growth, decay, and shedding of leaves). It remains difficult to represent the spatial-structural variability of

* Corresponding author: walter.box@aalto.fi

vegetation by a cylindrical approach [2]. Therefore, approaches incorporating the flexibility-induced reconfiguration and foliation have been proposed [3].

Due to experimental challenges, flow and sediment processes under complex combinations of channel geometry, vegetation types and sediments are less researched. The diversity of sediments and transport modes present in nature increases the effort needed. For instance, predictions of the transport and deposition of fine suspended sediment, such as cohesive particles (< 63 μm) and fine sand (< 200 μm), remain difficult in vegetated channels. Particular challenges arise when vegetation is present as a mixture of species, and when its density and coverage vary in space and time [4]. In fact, only a few studies [e.g. 3, 5, 6] have related deposition to hydraulically sound properties of natural vegetation.

For advancing the understanding of the transport, mixing and deposition of suspended sediment under complex conditions, reliable data of the local suspended sediment concentrations (SSC) are needed [7, 8]. Recent experiences indicate that this spatial and temporal variation of SSC can be measured at good accuracy e.g. by optical turbidity sensors or acoustic sensors in hydraulic flumes [e.g. 9, 10]. However, properties such as the size, shape, colour, and material of particles, plant disturbances, flume boundary reflections, and the effect of the relatively large turbidity probes on the flow field affect the reliability of the sensor-based SSC estimates. Therefore, the use of optical turbidity sensors in flume investigations requires careful consideration.

The goal of the present research project is to explore suspended sediment transport processes within a partly vegetated channel consisting of low grasses and flexible woody foliated vegetation. The specific objectives are to:

I) Quantify spatial distributions of suspended sediment concentration in case of flexible vegetation in a partly vegetated channel.

II) Characterize spatial variability of net deposition with a view on experimental repeatability within vegetated flume experiments.

III) Validate the use of optical backscatter turbidity sensors to measure SSC of fine silica sand expected to represent SS transport conditions of vegetated lowland channels.

Below we report first results of an ongoing flume study focusing on the case of submerged flexible grassy vegetation using ADV data of flow field, optical backscatter measurements of SSC, and weight-based deposition data collected from patches of vegetation. The scope of this study is on the non-cohesive sediment processes.

2. Methods

2.1. Flume properties and hydraulic conditions

Experiments were conducted at the Aalto Environmental Hydraulics Lab (EHL) using the 20 m long Environmental Hydraulics Flow Channel. The glass-walled working section of the flume is 16 m long, 0.6 m wide, and 0.8 deep (Fig. 1a). The flume was designed so that fine sediment particles are circulated and retained in motion. All experimental runs were conducted within steady and quasi-uniform flow conditions. A weir at the downstream end of the working section controlled the water depth, which was kept constant at 0.17 m. Water depths were measured by pressure sensors and manual point gauges. Discharge was measured by a magnetic flow meter. For the present experiments, one flow rate (180 m^3/h or 50 l/s) was used resulting in average streamwise velocities of 0.6 and 0.5 m/s in the open channel and vegetated part of the channel, respectively.

The flow field was determined in the fully developed part of the flow with an acoustic Doppler velocimeter, Nortek Vectrino+. We recorded vertical profiles at y = 130 and y = 250 mm to characterize the flow within and above the flexible grasses and a lateral transect at the

relative depth of 0.6 (z = 95 mm) to characterize the lateral shear layer formed between the unvegetated and the grassed parts of the channel. Both down- and side-looking ADV probes were used to obtain data close to the surface, bed and flume walls. For measuring points inside the vegetation, the grass stems were cleared from a circular area with a diameter of ca. 10 mm after all the other points were measured. Each measurement was conducted at the frequency of 200 Hz for a duration of 120 s. The Velocity Signal Analyser software [11] was used to filter out data with a signal-to-noise ratio < 17 and to de-spike the dataset using the modified phase-space threshold method [12]. Basic parameters of the mean and turbulent flow were computed, including the point mean velocity (u), depth-averaged mean velocity (U), turbulent kinetic energy (k), turbulence intensity (I), and lateral Reynolds stress (τ_{xy}).

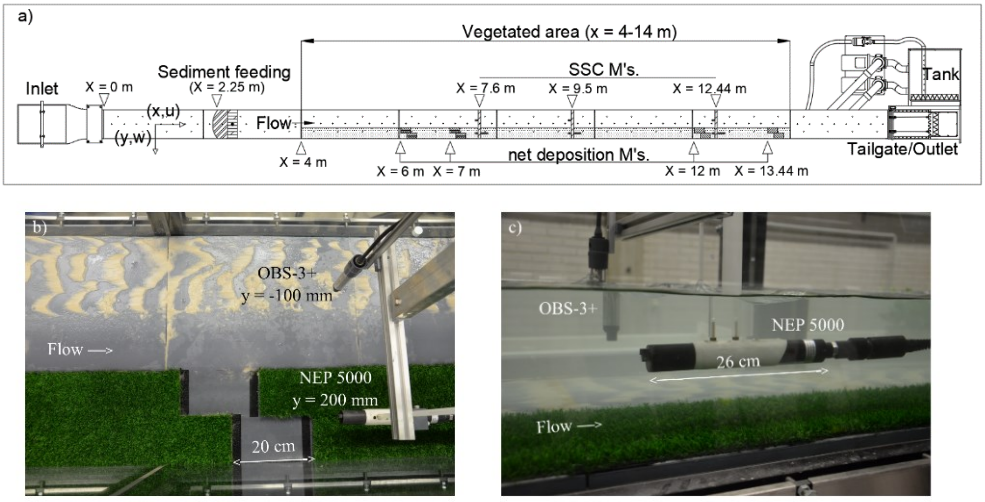

Fig. 1. a) Top view of the recirculating flume with the measurement positions denoted as M's b) the location of the removable measurement strips at x = 7.04 m, the positioning of the OBS-3+ and NEP5000 turbidity sensors at x = 7.6 m and y = -100 and y = 200 mm, respectively, and c) the turbidity sensors operating under flow.

2.2. Vegetation properties

A 10 m long and 0.23 m wide patch of artificial flexible vegetation was installed 4 m downstream of the start of the working section. The vegetation was attached on 15 mm thick PVC plates that covered the entire flume width. The artificial plants were selected to represent similar flexibility and reconfiguration behaviour as natural floodplain grasses. The grassy vegetation cover was on average 20 mm tall and consisted of 0.8 mm wide grass stems having a uniform stem density of ~65 stems/cm^2. The estimated bulk frontal area per volume was approximately 5 cm^{-1}.

2.3. Sediment properties

We selected natural silica quartz with a narrow particle size distribution and a complex-shaped geometry to ensure that the sediment was transported as individual particles not exhibiting cohesive behaviour. According to the manufacturer, the Sibelco S90 sand consists of silicate oxide (SiO_2, 99.5 mass/volume-%), the particles are flat to angular shaped and have a solid density (ρ_p) of 2.65 g/cm^3 and a dry bulk density of 1.4 g/cm^3. 99.9% of the particles were larger than 63 µm, 2.9% within 63-90 µm, 87% was within 90-180 µm and 10% within 180-250 µm. The median diameter (D_{50}) of the particles is 150 µm, the D_{10}, and

the D_{90} are 110 and 160 μm, respectively. Corresponding settling velocities (w_s) were estimated to be 0.011, 0.015, and 0.017 m/s for the D_{10}, D_{50}, and D_{90} sized particles, respectively. These estimates were derived using a force balance approach in combination with Stokes' law. We used a shape factor ϕ~2 for the angular sediment to determine the particle Reynolds number. The particle size distribution of the sediment was considered reasonably to represent transport processes in vegetated lowland channels, where suspended transport dominates. Visual observations indicated that deposited sand was intermittently transported as bed load in the unvegetated part of the flume due to the smooth bed (Figure 1b-c).

2.4. Turbidity sensors calibration and SSC measurements

Suspended sediment concentrations were measured with two different types of turbidity sensors, a Campbell OBS-3+ backscatter sensor and the Analite NEP5000 90° modulated infra-red (ISO7027) sensor. The OBS-3+ sensor optics are directed perpendicular to the length of the sensor. The lower range of the sensor (0-250 NTU) was selected with a manufacturer-stated accuracy of 4% or 10 mg/l for sandy material. The NEP5000 sensor optics were directed along the length of the sensor with the measurement range set at 0-10 NTU and has a manufactured-stated accuracy of 1-2%. The NEP5000 had a built-in wiper operating every 30 s, whereas the OBS-3+ was manually cleaned. The turbidity sensors were firmly attached to a metal arm, with the ability to move the sensors in the x, y and z directions (Fig. 1b). The sensors were placed so that the sensors optics were facing in the upstream direction of the flow. Both sensors were connected to a National Instruments USB-N6218 datalogger controlled with the NI SignalExpress software. The NEP5000 was configured to measure with a 5 Hz interval, and the OBS-3+ sensor operated at the maximum rate of 10 Hz. The turbidity sensors were calibrated within the flume without vegetation for five different SSC ranging from 1-176 mg/l. Flow and light conditions were kept constant while feeding the flume with the sediments at different rates (0, 2.4, 6.3, 8.6 and 12 g/s). Both sensors exhibited a high linearity and correlation ($R^2 = 0.99$ for the NEP5000 and $R^2 = 0.96$ for the OBS-3+) between the sensor output (voltage) and SSC. SSC were determined from filtered (mesh size of 34 μm) and dried 950 ml samples taken by a ISCO-6712 auto sampler. Statistical averages of raw sensor output (V) over 30-second time series were computed to derive the linear relations for the OBS-3+ and NEP5000 sensor.

SSC measurements were conducted at three longitudinal positions at x = 7.6, 9.5 and 12.44 m at y = -100 and y = 200 mm with the OBS-3+ and NEP5000, respectively. All measurements were taken at a depth of 9.5 cm. Statistical averages of 60-second time series of the voltage outputs were computed and converted by the use of the linear relations to derive corresponding SSC.

2.5. Experimental runs and net deposition measurements

Data for two 30-minute experimental runs were included in the present analyses. A total amount of 7 and 3.5 kg of the fine silica sand were added to the flume using the sediment feeding system (at x = 2.25, Fig. 1a). The sediment feeding rates were ~4.3 and ~2.4 g/s, respectively. The sediments were evenly distributed over the lateral direction of the flume using a conical shaped smooth surfaced plate with free fall in the water ~0.25 m above the water surface.

Net deposition measurements were conducted by a weight-based sampling approach. For this, removable rectangular grassed strips were used in the flume. The strips were 20 cm long and 5.6 or 11.2 cm wide with corresponding surface areas of 112 cm^2 and 224 cm^2, respectively. At the end of an experimental run the flume was slowly drained and the strips

were carefully removed and washed to collect the deposited sediments. Using this approach, net deposition was determined at four longitudinal locations (x = 6.04, 7.04, 12.04 and 13.54 m) (Fig. 1a). At the two most upstream locations (x = 6.04 and 7.04 m) four measurement strips were placed in a staggered pattern over the lateral direction of the vegetated patch, whereas at the downstream locations (x = 12.04 and 13.54 m) two larger strips (224 cm^2) were placed in a staggered pattern over the lateral (Fig. 1b).

3. Results and discussion

3.1. Mean and turbulent flow field

Figure 2 presents the vertical distributions of the key flow parameters at two lateral positions (y = 130 and 250 mm) in the vegetated part of the cross-section. The mean flow velocities were higher at y = 130 mm situated 60 mm from the vegetation edge compared to y = 250 mm which is located farther from the vegetation edge, 50 mm away from the flume wall (Fig. 2). When scaled with the depth-averaged velocity, the two vertical profiles collapsed together (Fig. 2). As expected, the profiles show very low velocities inside the dense grassy vegetation (z < 20 mm), relatively uniform velocities around the middle of the water column, and a velocity dip close to the surface caused by the small width-to-depth ratio of flume (3.5). The velocity dip was larger at y = 250 mm located closer to the flume wall, in accordance with e.g. [13].

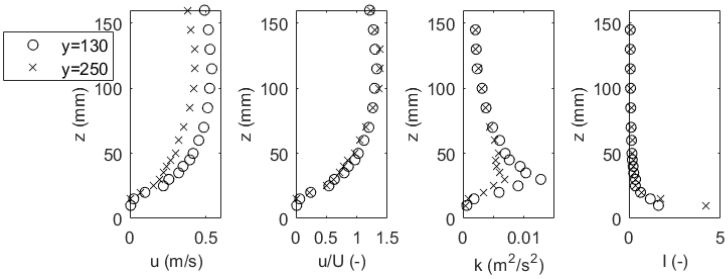

Fig. 2. Vertical profiles of mean velocity (u), mean velocity scaled by depth-averaged mean velocity (u/U), turbulent kinetic energy (k), and turbulence intensity (I) in the grassed part of the cross-section (at y = 130 and 250 mm) in the fully developed region of the flow at x = 11.66 m. The grasses extended from z = 0 to z = 20 mm.

Turbulence analyses showed that the vertical pattern of turbulence in the vegetated part of the cross-section was dominated by the vertical shear layer formed between the grass and the free overflow. For both vertical profiles, the turbulent kinetic energy (k) peaked at the depth of 30 mm, i.e. 10 mm above the top of the vegetation (Fig. 2), with the turbulent intensity reaching values of 0.3-0.4. Overall, the vertical profiles indicated a typical mixing-layer-type flow forming around the top of the vegetation, including an inflection point in the mean velocity profile, as is known to exist at the interface between dense plant stands and free overflow, e.g. [14].

Figure 3 shows the transversal distribution of the mean flow, lateral Reynolds stress, turbulent kinetic energy and turbulence intensity at the relative depth of 0.6, i.e. at z = 95 mm. Flow velocities were larger in the open channel (~0.6 m/s) compared to the vegetated part of the cross-section (~0.5 m/s). Excluding a 100 mm width near both flume walls due to the wall effects, the lateral Reynold stresses were largest at the interface between the vegetation and main channel, as can be expected for such a channel composed of two lateral regions differing in vegetative drag and roughness, e.g. [15]. These results indicated that

lateral turbulent transport of suspended sediment occurred between the main channel and the grassed part of the cross-section. Furthermore, turbulent kinetic energy was highest at the interface, while turbulence intensity was around 2 times larger over the vegetation and the lateral shear layer compared to the part of the open channel located outside the lateral shear layer, at y < -100 mm.

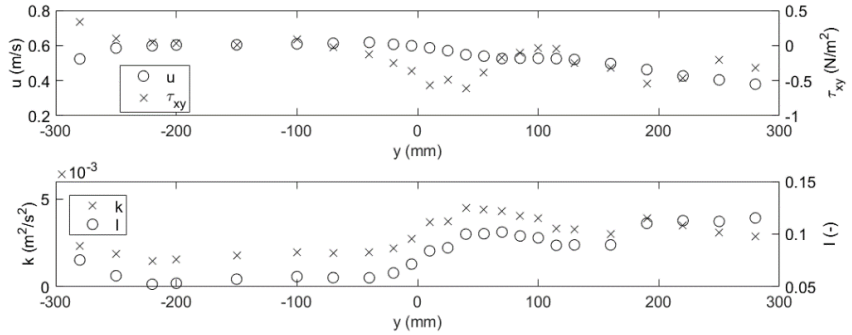

Fig. 3. Transversal profiles of velocity (u), lateral Reynolds stress (τ_{xy}), turbulent kinetic energy (k), and turbulence intensity (I) above the vegetation at the relative depth of 0.6 (z = 95 mm) in the fully developed flow region at x = 11.66 m. Grassy vegetation extended from y = 70 mm to y = 300 mm.

3.2. Spatial distribution of SSC

Data from the SSC measurements over the longitudinal direction of the flume from the two 30-minute runs with feeding at 4.3 and 2.4 g/s are shown in Figure 4. Corresponding background levels of SSC (at x = 7.6 m) at the start of the experimental runs (t = 0-150 s) were ~100 and 70 mg/l, respectively. The maximum measured SSC (at x = 7.6) in the experimental run with sediment feeding with 4.3 g/s was 65 and 100 mg/l of for the OBS-3+ and NEP5000 sensor, respectively. The minimum SSC measured was 35 and 50 mg/l at x = 12.44 m for the OBS-3+ and NEP5000, respectively. Overall, there was a strong decrease of SSC in the streamwise direction in both lateral positions located in the open channel (at y = -100 mm) and vegetated part (y = 200 mm) of the cross section. This rapid decrease of SSC was likely due to rapid settling of particles, so that the share of settled particles (or particles transported as bed-load) was higher for downstream locations. This pattern was less pronounced in the experimental run with the lower feeding rate (2.4 g/s). This was likely due to relatively high measurement uncertainties of SSC at the lower ranges of the turbidity sensors. In the unvegetated parts of the channel, sediment movement was observed as a combination of saltation, rolling, sliding, and moving Barchan type of dunes (Fig. 1b), but detailed analyses are beyond the scope of the present contribution. The interplay between settling, bed-load transport and resuspension can influence SSCs and indirectly net deposition measurements within the vegetation [e.g. 16, 17].

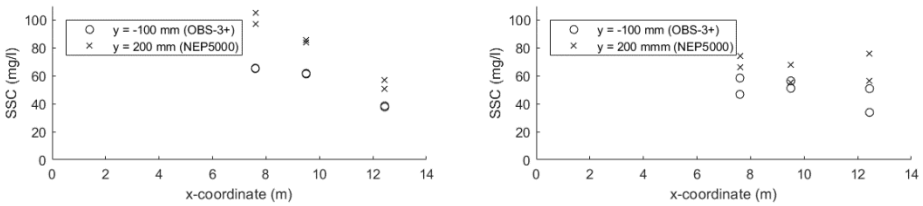

Fig. 4. Longitudinal pattern of SSC at y = -100 mm and y = 200 mm measured with the OBS-3+ and NEP5000 sensor, respectively for two different feeding rates, 4.3 g/s (left) and 2.4 g/s (right), with two replicate measurements conducted for each feeding rate.

3.3. Longitudinal pattern of net deposition

Net deposition per unit area (g/cm^2) on the removable strips at the end of the 30-minute duration experimental runs is shown in Figure 5. Maximum net deposition per unit area was 0.23 g/cm^2 and 0.06 g/cm^2 at x = 6.04 m for the experimental runs with the feeding rates of 4.3 and 2.4 g/s, respectively. Overall, the rate of net deposition was rapidly decreasing in the streamwise direction. This increase of cumulative net deposition with distance from the start of the vegetation coincides with comparable patterns observed previously [e.g. 1, 16, 17]. There was an absence of features indicating resuspension of bed-load transported sediment within the open channel, and settled particles within the dense bottom grass remained at their initial deposited position during the entire length of an experimental run despite the large turbulent flow structures above the grass. This in combination with low flow velocities (< 0.03 m/s) at the bed indicates that the depositional patterns were a result of suspended transport processes only. Some variation of net deposition in the lateral direction was observed, e.g. 0.16-0.24 and 0.03-0.09 g/cm^2 at x = 6 m in the experimental runs with feeding at 4.3 and 2.4 g/s, respectively. This was likely due to preferential deposition as a result of the flow field over the lateral direction of the vegetated cross section and due to errors resulting from the measurement procedure involving flushing, drying, and weighting uncertainties.

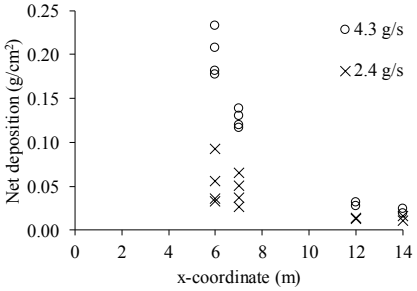

Fig. 5. Net deposition per unit area at four longitudinal positions (x = 6.04, 7.04, 12 and 13.54 m) at the end of the 30-minute duration experimental runs with corresponding feeding rates of 4.3 and 2.4 g/s.

4. Concluding remarks

First results from the ongoing research on transport and deposition of fine sandy sediment in a channel partly covered by flexible grassy vegetation were reported. The flow field exhibited a vertical mixing layer on top of the grasses and a lateral shear layer at the interface between the vegetated and non-vegetated parts of the channel width. The turbulent flow structure suggested that lateral turbulent transport of suspended sediment occurred between the main channel and the grassed part of the cross-section. From the measuring point of view, the experiments demonstrated that new-generation optical turbidity sensors were capable of providing scientifically useful SSC distribution data for fine suspended sand. Further experiments will be conducted to investigate interactions between the turbulent flow characteristics, SSC, and net deposition for a combination of grassy understory and flexible woody foliated vegetation.

We gratefully acknowledge the help of laboratory technician Antti Louhio and the preliminary work done by PhD student Gerardo Caroppi. The research was funded by Maa- ja vesitekniikan tuki ry (No 36537 and 33271) and by Maj and Tor Nessling Foundation (No 201800045).

References

1. L. Zong and H. Nepf, Geomorphology, *Flow and deposition in and around a finite patch of vegetation*, **116**, 363–372 (2010).
2. A. Vargas-luna, A. Crosato, G. Calvani, and W.S.J. Uijttewaal, Advances in Water Resources*, Representing plants as rigid cylinders in experiments and models*, **93**, 205–222 (2016).
3. K. Västilä and J. Järvelä, J. Soils Sediments, *Characterizing natural riparian vegetation for modeling of flow and suspended sediment transport*, 1–17 (2017).
4. J. Järvelä, J. Hydrol., *Effect of submerged flexible vegetation on flow structure and resistance*, **307**, 233–241 (2005).
5. C.I. Thornton, S.R. Abt, and W.P. Clary, Journal of the American water resources assosiation, *Vegetation influence on small stream siltation*, **33**, 1279–1288 (1998).
6. D. Corenblit, J. Steiger, A.M. Gurnell, E. Tabacchi, and L. Roques, Earth Surf. Process. Landforms, *Control of sediment dynamics by vegetation as a key function driving biogeomorphic succession within fluvial corridors*, **1810**, 1790–1810 (2009).
7. S. Temmerman, G. Govers, P. Meire, and S. Wartel, Mar. Geol., *Modelling long-term tidal marsh growth under changing tidal conditions and suspended sediment concentrations, Scheldt estuary, Belgium*, **193**, 151–169 (2003).
8. A.F. Lightbody and H.M. Nepf, Limnol. Oceanogr., *Prediction of velocity profiles and longitudinal dispersion in salt marsh vegetation*, **51**, 218–228 (2006).
9. K. Vastila, J. Jarvela, and H. Koivusalo, J. Hydraul. Eng., *Flow-Vegetation-Sediment Interaction in a Cohesive Compound Channel*, **142** (2016).
10. F. Ganthy, L. Soissons, P.-G. Sauriau, R. Verney, and A. Sottolichio, Sedimentology, *Effects of short flexible seagrass Zostera noltei on flow, erosion and deposition processes determined using flume experiments*, **62**, 997-1023, (2014).
11. M. Jesson, M. Sterling, and J. Bridgeman, Flow Meas. Instrum., *Despiking velocity time-series-Optimisation through the combination of spike detection and replacementmethods*, **30**, 45–51 (2013).
12. M. Parsheh, F. Sotiropoulos, and F. Porté-Agel, J. Hydraul. Eng., *Estimation of Power Spectra of Acoustic-Doppler Velocimetry Data Contaminated with Intermittent Spikes*, **136**, 368–378 (2010).
13. S. Yang, S. Tan, and S. Lim, J. Hydraul. Eng., *Velocity Distribution and Dip-Phenomenon in Smooth Uniform Open Channel Flows*, **130**, 1179–1186 (2005).
14. M. Ghisalberti and H. Nepf, Environ. Fluid Mech., *The structure of the shear layer in flows over rigid and flexible canopies*, **6**, 277–301 (2006).
15. B.L. White and H.M. Nepf, Water Resour. Res., *A vortex-based model of velocity and shear stress in a partially vegetated shallow channel*, **44**, 1–15 (2008).
16. R.G. Sharpe and C.S. James, Water SA, *Deposition of sediment from suspension in emergent vegetation*, **32**, 211–218 (2006).
17. E. Follett and H. Nepf, Estuaries and Coasts, *Particle Retention in a Submerged Meadow and Its Variation Near the Leading Edge*, 1–10 (2017).